JACS
JOURNAL OF THE AMERICAN CHEMICAL SOCIETY

COMMUNICATION

pubs.acs.org/JACS

Remarkable Enhancement in Thermoelectric Performance of BiCuSeO by Cu Deficiencies

Yong Liu,[†,‡] Li-Dong Zhao,[‖,*] Yaochun Liu,[§] Jinle Lan,[†] Wei Xu,[⊥] Fu Li,[†] Bo-Ping Zhang,[§] David Berardan,[‖] Nita Dragoe,[‖] Yuan-Hua Lin,[†,*] Ce-Wen Nan,[†,*] Jing-Feng Li,[†] and Hongmin Zhu[‡]

[†]State Key Laboratory of New Ceramics and Fine Processing, Department of Materials Science and Engineering, Tsinghua University, Beijing 100084, China

[‡]School of Metallurgical and Ecological Engineering and [§]School of Materials Science and Engineering, University of Science and Technology Beijing, Beijing 100083, China

[‖]Laboratoire d'Etude des Matériaux Hors Equilibre, Institut de Chimie Moléculaire et des Matériaux d'Orsay (CNRS UMR 8182), Univ. Paris Sud, Orsay F91405, France

[⊥]Beijing Synchrotron Radiation Facility, Institute of High Energy Physics, Chinese Academy of Sciences, Beijing, 100049, China

S *Supporting Information*

ABSTRACT: A significant enhancement of thermoelectric performance in layered oxyselenides BiCuSeO was achieved. The electrical conductivity and Seebeck coefficient of BiCu$_{1-x}$SeO (x = 0−0.1) indicate that the carriers were introduced in the $(Cu_2Se_2)^{2-}$ layer by Cu deficiencies. The maximum of electrical conductivity is 3×10^3 S m^{-1} for Bicu$_{0.975}$Seo at 650 °C, much larger than 470 S m^{-1} for pristine BiCuSeO. Featured with very low thermal conductivity (~0.5 W m^{-1} K^{-1}) and a large Seebeck coefficient (+273 μV K^{-1}), ZT at 650 °C is significantly increased from 0.50 for pristine BiCuSeO to 0.81 for BiCu$_{0.975}$SeO by introducing Cu deficiencies, which makes it a promising candidate for medium temperature thermoelectric applications.

Thermoelectric (TE) effects involve direct conversion between thermal and electrical energy by employing electrons and holes as energy carriers. Such effects are potential applications in power generation and electronic cooling.[1−3] The TE conversion efficiency can be well characterized by the dimensionless figure of merit $ZT = S^2\sigma T/\kappa$, where S, σ, κ, and T are the Seebeck coefficient, electrical conductivity, thermal conductivity, and absolute temperature, respectively. Therefore, a high electrical conductivity, large Seebeck coefficient, and low thermal conductivity are necessary for practical development of TE materials and related devices. Many alloys and oxides have been developed as TE materials. Yet, although many promising oxide-based systems, such as $Ca_3Co_4O_9$-based ($ZT \approx 0.2$ at 800 °C),[4,5] $NaCo_2O_4$-based ($ZT \approx 1$ at 527 °C, single crystals),[6,7] $SrTiO_3$-based ($ZT \approx 0.36$ at 1000 °C),[8] and In_2O_3-based ($ZT \approx 0.45$ at 1000 °C)[9,10] have been widely investigated over the past decades, their ZT values still remain low, which limits the applications of TE oxides. The low performance in oxides can be ascribed to the moderate electrical conductivity (~100−200 S·cm^{-1}) and high thermal conductivity (~3−10 W·m^{-1}·K^{-1}).

Recently, layered oxyselenides *Ln*Cu*Ch*O (*Ln*: La, Ce, Nd, Pr, Bi, and In; *Ch*: S, Se, and Te)[11−18] have been found to exhibit intriguing electrical transport properties. In analogy with high temperature superconductors, the exotic transport behaviors are grounded in the unique layered structure.[19] For example, BiCuSeO is composed by alternately stacking the insulating oxide $(Bi_2O_2)^{2+}$ layer acting as charge reservoir and the conductive selenide $(Cu_2Se_2)^{2-}$ layer constituting a conduction pathway for carrier transport, which is quite similar to other layered systems like Co-based oxides or iron-based superconductors.[20−23] Pristine BiCuSeO exhibits a low electrical conductivity (e.g., ~400 S m^{1-} at 50 °C);[22] however, a very recent report indicated that BiCuSeO based compounds with a band gap of 0.80 eV showed an excellent charge transport behavior due to the introduction of hole carriers by replacing Bi^{3+} with Sr^{2+} in the insulating $(Bi_2O_2)^{2+}$ layer, resulting in a high ZT, i.e., ZT = 0.76.[24] Thus, an interesting issue arises: can the TE performance of BiCuSeO also be enhanced by directly introducing holes into the conductive selenide $(Cu_2Se_2)^{2-}$ layers?

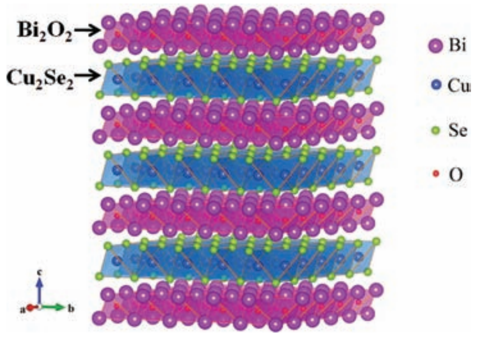

Figure 1. Crystal structure of BiCuSeO with ZrSiCuAs-type tetragonal structure (*P*4/*nmm* space group).

Here, we report a successful route to achieve high TE performance by introducing Cu deficiencies in the $(Cu_2Se_2)^{2-}$ layers. With highly improved electrical conductivity but maintaining a relatively high Seebeck coefficient and low thermal conductivity, high TE performance is achieved with ZT up to 0.81 at 650 °C, which is nearly two times larger than that of the pristine BiCuSeO.

Received: September 28, 2011
Published: November 15, 2011

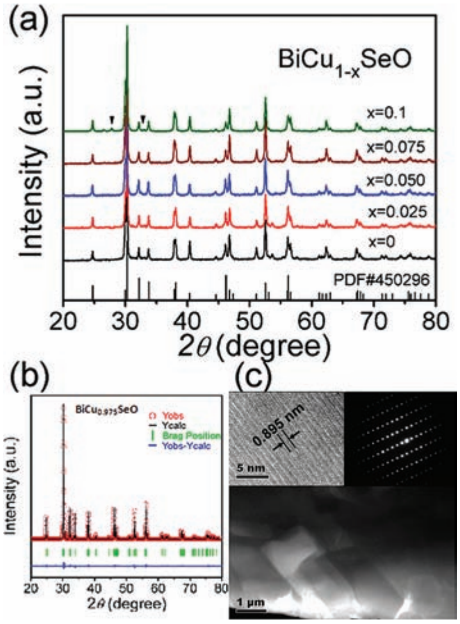

Figure 2. (a) XRD patterns for $BiCu_{1-x}SeO$. (b) Rietveld refinement of $BiCu_{0.975}SeO$, and (c) TEM of $BiCu_{0.975}SeO$.

As shown in Figure 1, the structure of BiCuSeO is composed of alternating PbO-like $(Bi_2O_2)^{2+}$ and anti-PbO-like $(Cu_2Se_2)^{2-}$ layers stacked perpendicular to [0 0 1]. These layers are built from edge-sharing [OBi4] and tetrahedral [CuSe4], respectively.

The experimental details can be found as Supporting Information. By introducing Cu deficiencies, series $BiCu_{1-x}SeO$ samples were prepared using a two-step solid state reaction route as described in the following reaction equation:

$$Bi + (3 - 3x)Cu + 3Se + Bi_2O_3 = 3BiCu_{1-x}SeO \quad (1)$$

All the peaks can be indexed as a major phase BiCuSeO (PDF#45-0296) except a minor Bi_2O_3 impurity phase (see, for example, at $2\theta = 28°$ and $2\theta = 33°$) as the Cu deficiency level increases to 0.10, as shown in Figure 2a. The results indicate that a Cu deficiency of ≥ 0.1 cannot be guaranteed due to the instability of Bi and Se rich phases. The relative densities of these samples range from 99.2% to 97.4%. Figure 2b shows the Rietveld refinement of $BiCu_{0.975}SeO$. The agreement between the experimental data (red circle) and the calculations (black line) is good, and the R_{wp} (weighted residual error, blue line) factor is about 5.4%; the other typical R values for all refinements are $R_p \approx 4.1\%$ and $R_{Bragg} \approx 1.8\%$. Rietveld refinement illustrates that lattice parameters (a and c) decrease with increasing Cu deficiencies (Figure S1), and Hall coefficients measurements observed that carrier concentration is increased with increasing deficiencies, which indicate that Cu deficiencies are artificially introduced. The TEM micrograph (Figure 2c) for the $BiCu_{0.975}SeO$ bulk sample prepared illustrates an ~1 μm grain size, and the distance of the lattice in HRTEM is consistent with the c lattice parameter. It is noted that XRD patterns (Rietveld refinement) both perpendicular and parallel to the spark plasma sintering (SPS) pressing direction do not evidence any obvious preferential orientation of the crystalline particles. Therefore, the TE transport properties for $BiCu_{1-x}SeO$ polycrystals prepared by SPS with ball milling powders can be assumed as isotropic.

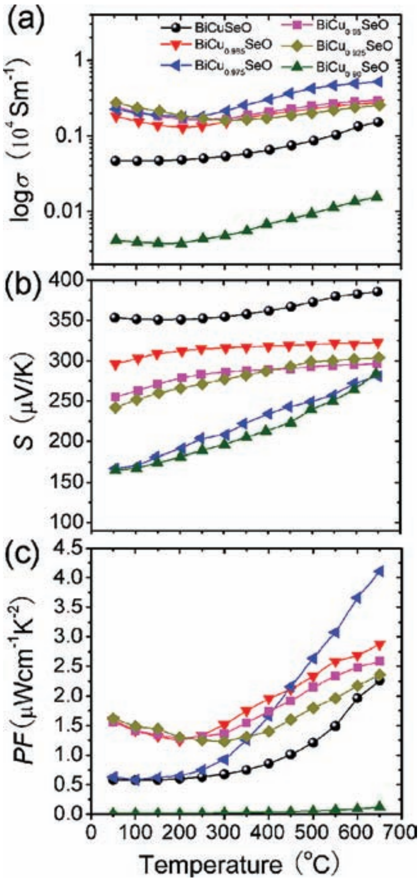

Figure 3. Temperature dependence of (a) electrical conductivity, (b) Seebeck coefficient, and (c) power factor of $BiCu_{1-x}SeO$ ceramics.

The temperature dependence of the electrical conductivity for the $BiCu_{1-x}SeO$ samples is shown in Figure 3a. Pristine BiCuSeO exhibits low electrical conductivity values over the entire measuring temperature range. By contrast, the samples with a Cu deficiency ($x < 0.1$) show a significantly enhanced electrical conductivity. For example, the electrical conductivity of $BiCu_{0.975}SeO$ is 5.3×10^3 S m^{-1} at 650 °C, 1 order of magnitude higher than 470 S m^{-1} of pristine BiCuSeO. As the Cu deficiency exceeds 0.1, the $BiCu_{0.90}SeO$ sample shows the lowest electrical conductivity, which results from the drop in carrier mobility (Table S1) that may be related to the presence of Bi_2O_3 impurity phases as identified in the XRD patterns. The enhanced electrical conductivity of $BiCu_{1-x}SeO$ with $x < 0.1$ can be attributed to the hole carriers, which are induced by introducing Cu deficiencies in the charge conductive selenide $(Cu_2Se_2)^{2-}$ layers; this can be explained by a defect equation as follows:

$$2BiCu_{1-x}SeO = (Bi_2O_2)^{2+} + (Cu_{2(1-x)}Se_2)^{(2+x)-} + xV_{Cu}^{-} + 2xh^{+} \quad (2)$$

where V_{Cu}^{-} is the Cu vacancy, and h^+ the produced holes. This means that the hole concentration can be increased by introducing acceptor Cu deficiencies. (Table S1).

The Cu deficiencies also have a significant effect on the Seebeck coefficients, as shown in Figure 3 b. The positive Seebeck coefficients indicate a p-type electrical transport behavior. The Seebeck coefficient for BiCuSeO is large, e.g., +353 μV K^{-1}

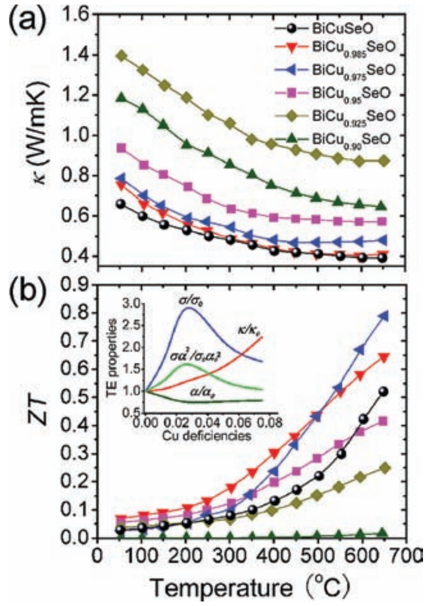

Figure 4. Temperature dependence of (a) thermal conductivity and (b) *ZT* of $BiCu_{1-x}SeO$ samples. The inset in (b) shows the normalized TE properties of $BiCu_{1-x}SeO$ samples at 650 °C as a function of *x*.

at 50 °C and +386 μV K^{-1} at 650 °C. Larger Seebeck coefficients could be related to its layered crystal structure, with insulating $(Bi_2O_2)^{2+}$ layers and conductive $(Cu_2Se_2)^{2-}$ layers alternately forming a natural superlattice, with a two-dimensional confinement of the charge carriers. Here, the natural layered structure of $(Bi_2O_2)^{2+}/(Cu_2Se_2)^{2-}/(Bi_2O_2)^{2+}$ is very similar to $SrTiO_3$/$SrTi_{0.8}Nb_{0.2}O_3$/$SrTiO_3$, which is typically composed of artificial layers of insulating/conductive/insulating, which exhibits a huge Seebeck coefficient.[25] Hosono and his co-workers performed a detailed calculation for DOS of BiCuSeO and revealed that a large Seebeck coefficient can be achieved in a *p*-type BiCuSeO.[14] Upon the formation of Cu deficiencies, the Seebeck coefficients decrease due to the increased hole concentration but is still maintained at +165 to +323 μV K^{-1} over the entire measuring temperature range. Similar behavior was also observed in LaCuSeO by Masuda et al.[22] The enhanced electrical conductivity and positive temperature dependent Seebeck coefficient cause all the power factors ($PF = S^2\sigma$) to peak at high temperature (2.36−4.10 μW cm^{-1} K^{-2} at 650 °C), as shown in Figure 3 c.

Figure 4a shows the thermal conductivity values for $BiCu_{1-x}SeO$. The thermal conductivity of pristine BiCuSeO decreases with increasing temperature, from ~0.70 W m^{-1} K^{-1} at 20 °C to ~0.40 W m^{-1} K^{-1} at 650 °C. Normally, the total thermal conductivity is the sum of the electronic and lattice contributions.[26−28] At room temperature, considering the Wiedemann−Franz law, the electronic contribution to the total thermal conductivity is estimated to be less than 0.35% for the pristine BiCuSeO sample and it increases only 5.40% at 650 °C. We also calculated the Lorenz number by derivation from the Fermi energy with a simple assumption of a single band gap model and acoustic phonon scattering. Our results reveal that the lattice thermal conductivities using both the calculated Lorenz number and the present constant (1.5×10^{-8} W Ω K^{-2}) show a similar change trend with increasing Cu deficiencies (Figure S4b−c). The results indicate that the phonon contribution is predominant. The low thermal conductivity of $BiCu_{1-x}SeO$ may originate from the layered structure since phonons can be scattered at the layers' interfaces,[29,30] from the weak bonding between layers,[31,32] from the presence of low-phonon-conductive heavy elements,[33] or from some other reasons. This is an open issue and needs further clarification. At $x = 0.1$ the thermal conductivity of the $BiCu_{0.90}SeO$ sample is lower than that of the $BiCu_{0.925}SeO$ sample, which could be due to phonon scattering by the Bi_2O_3 impurity phase in the $BiCu_{0.90}SeO$.

By using the electrical and thermal transport properties, the dimensionless figure of merit (*ZT*) is calculated as shown in Figure 4b. *ZT* increases with temperature, with the maximum *ZT* value at 650 °C being ~0.81 for the $BiCu_{0.975}SeO$ sample. This *ZT* of 0.81 is the highest value reported for bulk oxides so far. The comparison shown in the inset of Figure 4b (TE properties of pristine BiCuSeO were marked by the subscript symbol *o*) demonstrates that the present obtained high *ZT* is due mainly to improved electrical conductivity. The present work indicates that the TE properties of BiCuSeO can be remarkably improved by Cu deficiencies in the conductive selenide $(Cu_2Se_2)^{2-}$ layers.

In summary, the electrical transport properties of *p*-type $BiCu_{1-x}SeO$ ($x = 0-0.1$) were enhanced by introducing Cu deficiencies in the conductive selenide $(Cu_2Se_2)^{2-}$ layers. A low thermal conductivity and large power factor were achieved, resulting in a high *ZT* of 0.81 at 650 °C in $BiCu_{0.975}SeO$, which makes it a very promising candidate for thermoelectric applications.

■ ASSOCIATED CONTENT

Ⓢ Supporting Information. Experimental details, carrier mobility and carrier density (Table S1), lattice parameters (Figure S1), temperature dependence of thermal diffusivity (Figure S2), heat capacity (Figure S3), and lattice thermal conductivity (Figure S4). This material is available free of charge via the Internet at http://pubs.acs.org.

■ AUTHOR INFORMATION

Corresponding Author

zhao-lidong@hotmail.com; linyh@mail.tsinghua.edu.cn; cwnan@mail.tsinghua.edu.cn

■ ACKNOWLEDGMENT

This work was financially supported by the Ministry of Science and Technology of China through a 973-Project, under Grant No. 2007CB607505, NSF of China under Grant No. 51025205, and High-Tech 863 Program of China (Grant No. 2009AA03Z216). Scientific Research Project of Tsinghua University No. 20111080969, and Natural Science Fund of China under Grant No. 11220119.

■ REFERENCES

(1) DiSalvo, F. J. *Science* **1999**, *285*, 703.

(2) Rowe, D. M. *CRC Handbook of Thermoelectrics*: CPC Press: Boca Raton, FL, 1995;

(3) Snyder, G. J.; Toberer, E. S. *Nat. Mater.* **2008**, *7*, 105.

(4) Masuda, Y.; Nagahama, D.; Itahara, H.; Tani, T.; Seoc, W. S.; Koumotoa, K. *J. Mater. Chem.* **2003**, *13*, 1094.

(5) Wang, Y.; Sui, Y.; Cheng, J.; Wang, X.; Su, W. *J. Phys. D: Appl. Phys.* **2008**, *41*, 045406.

(6) Wang, Y.; Nyrissa, S.; Cava, R. J.; Ong, N. P. *Nature* **2003**, *423*, 425.

(7) Fujita, K.; Mochida, T.; , Nakamura, K. *Jpn. J. Appl. Phys.* Part 1, **2001**, *40*, 4644.

(8) Wang, H. C.; Wang, C. L.; Su, W. B.; Liu, J.; Zhao, Y.; Peng, H.; Zhang, J. L.; Zhao, M. L.; Li, J. C.; Yin, N.; Mei, L. M. *Mater. Res. Bull.* **2010**, *45*, 809.

(9) Berardan, D.; Guilmeau, E.; Maignan, A.; Raveau, B. *Solid State Commun.* **2008**, *146*, 97.

(10) Guilmeau, E.; Bérardan, D.; Simon, Ch.; Maignan, A.; Raveau, B.; Ovono Ovono, D.; Delorme, F. *J. Appl. Phys.* **2009**, *106*, 053715.

(11) Hiramatsu, H.; Ueda, K.; Takafuji, K.; Ohta, H.; Hirano, M.; Kamiya, T.; Hosono, H. *J. Appl. Phys.* **2003**, *94*, 5805.

(12) Yasukawa, M.; Ueda, K.; Hosono, H. *J. Appl. Phys.* **2004**, *95*, 3594.

(13) Ueda, K.; Takafuji, K.; Hiramatsu, H.; Ohta, H.; Kamiya, T.; Hirano, M.; Hosono, H. *Chem. Mater.* **2003**, *15*, 3692.

(14) Hiramatsu, H.; Yanagi, H.; Kamiya, T.; Ueda, K.; Hirano, M.; Hosono, H. *Chem. Mater.* **2008**, *20*, 326.

(15) Ueda, K.; Hosono, H.; Hamada, N. *Appl. J. Phys.* **2005**, *98*, 043506.

(16) Ueda, K.; Hiramatsu, H.; Ohta, H.; Hirano, M.; Kamiya, T.; Hosono, H. *Phys. Rev. B* **2004**, *69*, 155305.

(17) Inoue, S.; Ueda, K.; Hosono, H.; Hamada, N. *Phys. Rev. B.* **2001**, *64*, 245211.

(18) Hiramatsu, H.; Ueda, K.; Takafuji, K.; Ohta, H.; Hirano, M.; Kamiya, T.; Hosono, H. *Appl. Phys. A: Mater. Sci. Process.* **2004**, *79*, 1517.

(19) Terasaki, I.; Sasago, Y.; Uchinokura, K. *Phys. Rev. B.* **1997**, *56*, 12685.

(20) Pinsard-Gaudart, L.; Berardan, D.; Bobroff, J.; Dragoe, N. *Phys. Status Solidi RRL* **2008**, *2*, 185.

(21) Kamihara, Y.; Hiramatsu, H.; Hirano, M.; Kawamura, R.; Yanagi, H.; Kamiya, T.; Hosono, H. *J. Am. Chem. Soc.* **2008**, *130*, 3296.

(22) Masuda, Y.; Nagahama, D.; Itahara, H.; Tani, T.; Seoc, W. S.; Koumotoa, K. *J. Mater. Chem.* **2003**, *13*, 1094.

(23) Takahashi, Y.; Gotoh, Y.; Akimoto, J. *J. Solid State Chem.* **2003**, *172*, 22.

(24) Zhao, L.-D.; Berardan, D.; Pei, Y. L.; Byl, C.; Pinsard-Gaudart, L.; Dragoe, N. *Appl. Phys. Lett.* **2010**, *97*, 092118.

(25) Ohta, H.; Kim, S.; Mune, Y.; Mizoguchi, T.; Nomura, K.; Ohta, S.; Nomura, T.; Nakanishi, Y.; Ikuhara, Y.; Hirano, M.; Hosono, H.; Koumoto, K. *Nat. Mater.* **2007**, *6*, 129.

(26) Poudel, B.; Hao, Q.; Ma, Y.; Lan, Y.; Minnich, A.; Yu, B.; Yan, X.; Wang, D.; Muto, A.; Vashaee, D.; Chen, X.; Liu, J.; Dresselhaus, M. S.; Chen, G.; Ren, Z. *Science* **2008**, *320*, 634.

(27) Hsu, K. F.; Loo, S.; Guo, F.; Chen, W.; Dyck, J. S.; Uher, C.; Hogan, T.; Polychroniadis, E. K.; Kanatzidis, M. G. *Science* **2004**, *303*, 818.

(28) Rhyee, J.; Lee, K. H.; Lee, S. M.; Cho, E.; Kim, S. I.; Lee, E.; Kwon, Y. S.; Shim, J. H.; Kotliar, G. *Nature (London)* **2009**, *459*, 965.

(29) Venkatasubramanian, R.; Siivola, E.; Colpitts, T.; O'Quinn, B. *Nature* **2001**, *413*, 597.

(30) Hicks, L. D.; Dresselhaus, M. S. *Phys. Rev. B* **1993**, *47*, 12727.

(31) Zhao, L.-D.; Zhang, B. P.; Liu, W. -S.; Zhang, H. L.; Li, J.-F. *J. Solid State Chem.* **2008**, *181*, 3278.

(32) Chiritescu, C.; Cahill, D. G.; Nguyen, N.; Johnson, D.; Bodapati, A.; Keblinski, P.; Zschack, P. *Science* **2007**, *315*, 351.

(33) Clarke, D. R. *Surf. Coat. Technol.* **2003**, *163*, 67.